Chemical Engineering Journal 451 (2023) 138984

Contents lists available at ScienceDirect

Chemical Engineering Journal

journal homepage: www.elsevier.com/locate/cej

Experimental review of different plasma technologies for the degradation of cylindrospermopsin as model water pollutant

Marcel Schneider [a,b], Raphael Rataj [b], Luděk Bláha [a], Juergen F. Kolb [b,*]

[a] RECETOX, Faculty of Science, Masaryk University, Kotlarska 2, 61137 Brno, Czech Republic
[b] Leibniz Institute for Plasma Science and Technology (INP), Felix-Hausdorff-Straße 2, 17489 Greifswald, Germany

ARTICLE INFO

Keywords:
Active discharge volume
Advanced oxidation process
Cyanotoxin
Electric discharge
Non-thermal plasma
Water treatment

ABSTRACT

The challenge to remove more frequently occurring recalcitrant pollutants from drinking water has recently led to a rising interest for more advanced treatment. Non-thermal plasma was repeatedly introduced as a versatile method that can be adapted towards specific treatment needs. Nevertheless, investigations were so far focused on few or particular discharge configurations without thorough evaluation and comparison of their potential for different applications and especially the treatment of larger volumes. Therefore, we investigated six common but fundamentally different systems with respect to the degradation of a highly toxic compound of increasing concern, i.e. cylindrospermopsin. Accordingly, discharges either submerged in water, operated at the air–water interface or in air were appraised with respect to operating parameters and conditions. Their individual potential was assessed by the absolute degradation of the model compound and the time and energy required to remove 90 % of the toxin. The dissipated energy generally resulted in the generation of, to some extent, different reactive chemical species, which were found primarily responsible for the degradation. A dielectric barrier discharge in a water mist was the most versatile approach with the best performance regarding different criteria. A submerged corona-like discharge still offered a reasonable compromise between time and energy required to degrade the toxin by 90 % and even submerged spark discharges presented a viable option. The active discharge volume, describing the volume in which the dissipated energy can be effectively exploited, and the capacity to increase this volume was identified as a crucial scaling parameter for any configuration.

1. Introduction

Conventional water treatment methods are often ineffective for the removal of dissolved recalcitrant organic compounds [1,2]. Hence, advanced filtration methods, i.e. nanofiltration, reverse osmosis or activated carbon, are employed [1,3] or advanced oxidation processes (AOPs) considered [1,4]. The retention by filtration or adsorption requires subsequent processing of the highly contaminated retentate as well as periodical maintenance, including the laborious exchange and disposal of filter membranes or beds. Therefore, the actual degradation of the pollutants, e.g. by AOPs, is a preferable option. Especially the *in situ* production of hydroxyl radicals (·OH) provides a possibility for the degradation of persistent compounds. However, the radical is short-lived and an efficient generation and mixing in the treated water is needed. Consequently, providing other species instead, e.g. nitric oxide radicals (NO·), hydrogen peroxide (H_2O_2) or ozone (O_3), could be the more economical and sufficient approach for the remediation for many or most contaminants that are currently of concern for water treatment. The method of choice for the production and control of such reactive species is usually a non-thermal plasma (NTP) method, as it is for example already established for the ozonation of drinking water.

Plasma processes are inherently versatile and, depending on the design of the plasma source, can continuously generate a range of reactive species, including ·OH, H_2O_2, O_3, NO·, excited molecules, atoms and ions as well as electrons and photons. The discharge type and operating medium determine the type and amount of the produced reactive species [5,6]. Correspondingly, a plasma treatment can be selected and optimized towards specific water treatment applications. Reactive species that are interesting for water treatment, i.e. ·OH and O_3, can be directly generated from water and air, respectively. Since no additional precursor chemicals or catalysts are required, NTPs can be considered environmentally benign. Moreover, NTPs were shown to even degrade recalcitrant organic pollutants that were persistent or only somewhat susceptible to conventional and other advanced treatment

* Corresponding author at: Leibniz Institute for Plasma Science and Technology (INP), Felix-Hausdorff-Straße 2, 17489 Greifswald, Germany.
E-mail address: juergen.kolb@inp-greifswald.de (J.F. Kolb).

https://doi.org/10.1016/j.cej.2022.138984
Received 20 June 2022; Received in revised form 10 August 2022; Accepted 30 August 2022
Available online 6 September 2022

techniques [4].

An instructive example for the comparison of different methods with respect to efficacies and efficiencies is the rather stable cyanobacterial toxin cylindrospermopsin (CYN). The pollutant exemplifies an emerging threat to water reservoirs by natural toxins. Cyanobacteria, which are found in surface waters all around the globe, produce a range of toxic secondary metabolites known as cyanotoxins. In recent years, cyanobacterial blooms occurred more frequently due to increased eutrophication, which, in turn, also increased cyanotoxin occurrence and abundance [7]. These compounds are known for their stability against conventional water treatment methods [3]. They also proved resilient against some AOPs [8]. Consequently, a limited number of studies have explored the potential of NTPs and especially dielectric barrier discharges (DBDs) for the removal of cyanotoxins, e.g. anatoxin-a [9], β-*N*-methylamino-L-alanine [10], CYN [11] and microcystin-LR [12]. However, similar to investigations on other contaminants, a systematic comparison between principally possible but distinct NTP concepts for water treatment, with respect to efficacy and efficiency but also mechanisms of pollutant degradation as well as other aspects with implications for their implementation, has so far not been presented. Although some studies have already compared different discharge concepts, they either investigated modifications of rather similar electrode configurations, compared solely on the energy efficiency and/or evaluated the performance of various plasma reactors based on reports for different contaminants and treatment conditions [13–16].

The corresponding gap in knowledge was addressed by the presented study. Six different but often discussed discharge configurations were investigated using the same compound, i.e. CYN as an instructive model for a naturally occurring surface water pollutant. The six discharges were grouped into three categories based on operating media and operating principles: i) *submerged in water*: corona-like and spark discharges, ii) *at the air–water interface*: DBD and surface discharge, and iii) *in air*: arc discharge and plasma jet. Each of the different discharges exhibited distinguishable physico-chemical characteristics as well as advantages and disadvantages with respect to their application in drinking water treatment. The aim of this study was to investigate differences of the discharges and the implications for water treatment in more detail to provide a guideline for identifying the most promising reactor setups and discharge types for future research and development. Comparison of the different discharges was based on the degradation efficacy, economic feasibility, design characteristics with relevance to the scaled up implementation as well as potentially involved degradation mechanisms. The results are important with respect to natural toxins but moreover for the remediation of recalcitrant water pollutants by NTPs in general.

2. Materials and methods

2.1. Standard and reagents

Since a CYN standard in larger quantities is expensive, an extraction of CYN was adapted from Cerasino et al. [17]. In short, freeze-dried biomass of *Aphanizomenon flos-aquae* (PCC 7905) was extracted with 75 % methanol, sonicated on ice for 30 min and centrifuged at 3390 × g for 10 min. The extraction was repeated three times and supernatants were pooled. The methanolic extract was dried under N_2 at 45 °C, redissolved in Milli-Q water and centrifuged using 0.22 µm cellulose acetate spin filters (National Scientific) at 7380 × g for 10 min. 1 mg of dry CYN (≥95 %), obtained from Enzo Life Sciences, Inc., was dissolved in 1 mL methanol and used for calibration. Water (LC-MS Ultra Chromasolv™ for UHPLC-MS) was obtained from Honeywell™ Riedel-de Haën™. Methanol (Rotisolv® HPLC Gradient) and acetonitrile (Rotisolv® Ultra LC-MS grade) were purchased from Carl Roth and formic acid from Fluca Analytical.

The chemical structure of CYN is shown in Fig. 1. Oxidative degradation of CYN by, e.g. O_3, •OH or sulfate radical ($SO_4^{\bullet-}$) is often reported

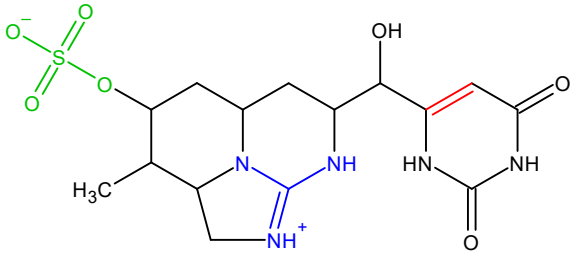

Fig. 1. Structure of cylindrospermopsin. Highlighted groups indicate structural features susceptible to oxidative degradation: C═C double bond in the hydroxymethyl uracil moiety (in red), guanidine structure (in blue), and sulfate group (in green).

to follow a similar pathway. The most susceptible sites to initiate the oxidative degradation of CYN are the C═C double bond of the hydroxylmethyl uracil moiety and the guanidine system, followed by the sulfate group (highlighted moieties in Fig. 1) [18,19].

2.2. Cylindrospermopsin quantification

Cylindrospermopsin was quantified by an Agilent 1200 Infinity Series HPLC coupled with an Agilent 1260 DAD detector (Agilent Technologies) at λ = 262 nm on an InfinityLab Poroshell 120 SB-AQ column (3 × 100 mm, 2.7 µm, Agilent Technologies) equipped with an InfinityLab Poroshell 120 SB-AQ guard column (3 × 5 mm, 2.7 µm, Agilent Technologies). Separation was achieved using gradient elution with acidified water (0.1 % formic acid) and acetonitrile at a flow rate of 0.7 mL min^{-1} and 10 µL injection volume (for details see Supplementary Table S1).

2.3. Plasma sources and treatments

Altogether six plasma concepts were investigated, which differed, on the one hand, in the underlying discharge processes and characteristics of the plasmas, e.g. temperatures, and on the other hand, in the way the contaminated water was treated. The principles can be categorized into plasmas that are generated directly in the water (submerged spark and corona-like discharges), plasmas that are established at and in interaction with the water surfaces (surface discharge and DBD in air with suspended water droplets) and discharges that are generated in air with their effluents mixed into water (arc discharge and plasma jet). The different approaches provided different reaction pathways, including the generation of different reactive species. The otherwise similar conceptual setup of the experiments, as shown in Fig. 2a, permitted the direct comparison of these methods. Photographs of the respective systems and the plasmas that were generated are shown in Supplementary Figures S1-S6. The plasma was generated by the application of either DC, sinusoidal or pulsed high voltages between 'active' high voltage and ground electrodes as described for each approach in the following paragraphs. Applied voltages and concurrent currents were monitored with a passive high voltage probe (P6015A, Tektronix) and current monitor (Model 2878, Pearson). Energies that were dissipated in the plasma were calculated by integration of applied voltages and associated currents. A water volume of 200 mL, containing a nominal concentration of 0.3 µg mL^{-1} of CYN, was circulated through the cooling system, the plasma reactor and back into the expansion reservoir, from which samples were taken for CYN quantification at different time points during the treatment of 60 min. If the plasma exposures were expected to be prone to increase water temperatures, the water temperature was controlled by the cooling system. Therefore, the cooling system was initially set to 7 °C. Since no significant increase of the solution temperature was observed after operating the corona-like and surface discharges for 60 min, the temperature was then set to 18 °C for the other discharges to resemble a temperature that can be measured in

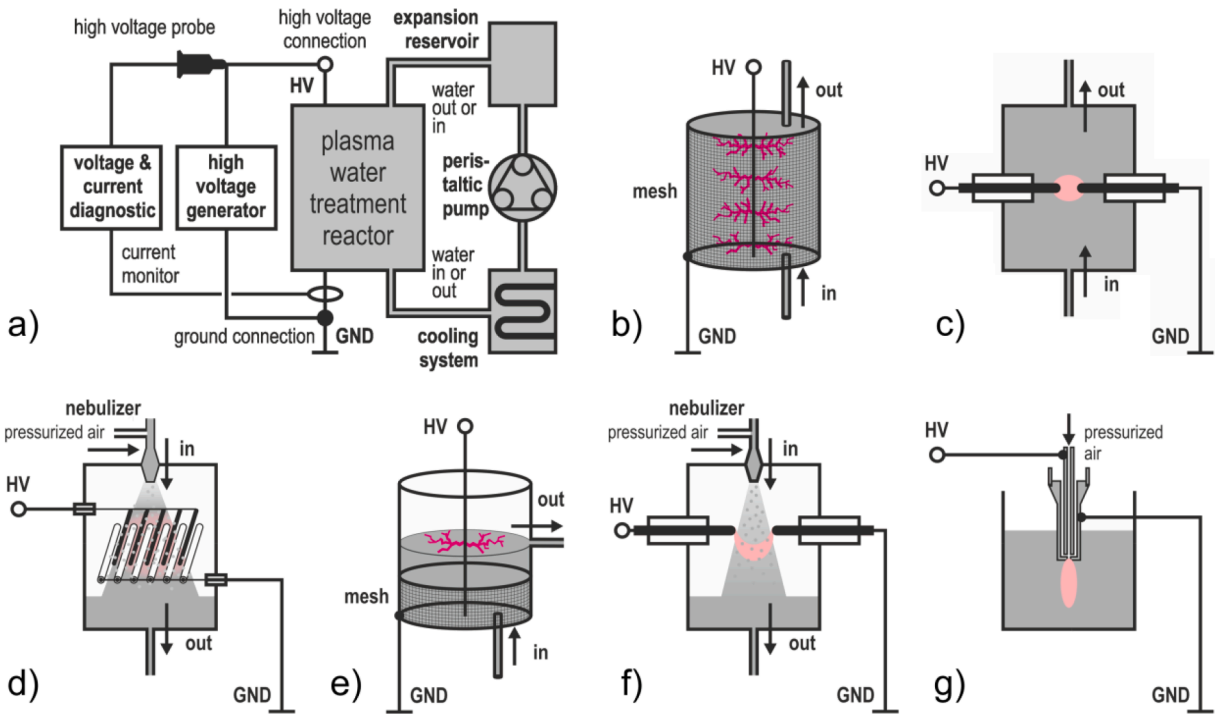

Fig. 2. a) Block diagram of the experimental setup for CYN degradation with six different plasma reactors: b) corona-like discharges in water, c) underwater spark discharges, d) DBDs in air around an aerosol, e) surface discharges at the air–water interface, f) arc discharges in air, and g) plasma jet submerged in water.

surface waters in summer, i.e. the season in which massive cyanobacterial blooms usually occur. The experiments were independently repeated twice. We refrained from increasing the number of iterations since we observed that this did not provide considerable additional insight with respect to the comparison of plasma sources, however, would have required significant additional effort and resources.

2.4. Corona-like discharges in water

Corona-like discharges were formed in water along the entire length of two intertwined 50 µm tungsten wires (99.95 %) at the center of the coaxial reactor, which were surrounded by a stainless steel mesh (0.5 mm mesh size, 200 µm wire diameter) at a distance of 17 mm and with a height of 40 mm. Discharges were generated by the application of positive high voltage pulses of 67.9 kV from a 6-stage Marx bank pulse generator operated at a frequency of 20 Hz. The reactor measured 70 mm in height and 34 mm in diameter and was completely filled with 64 mL of water, pumped from the bottom of the reactor to its top. The configuration is shown in Fig. 2b. The CYN solution was chilled to 7 °C and circulated at 50 mL min^{-1}. The concept has previously been successfully applied for the decomposition of pharmaceuticals in water [4].

2.5. Spark discharges in water

Spark discharges were generated directly in water between the tips of two sharpened tungsten rods with a diameter of 2 mm and with tips 0.5 mm apart, as shown in Fig. 2c. Positive high voltage pulses of 100 ns and 42 kV in amplitude were applied between the electrodes from a 6-stage Marx pulse generator at a frequency of 20 Hz. The CYN solution was pumped at 50 mL min^{-1} from the bottom of the 100 mm long reactor chamber through the electrodes and cooled to 18 °C. The reactor diameter of 6 mm was selected to increase the ratio between active plasma and reactor volume. The approach has been studied for the disintegration of microalgae but also for pollutant degradation [20,21].

2.6. Dielectric barrier discharge in humid air with immersed water droplets

Dielectric barrier discharges were established in humid air with water droplets by the application of negative high voltage pulses with a duration of 400 ns and negative amplitude of −10.7 kV that were provided from a pulse generator (Eagle Harbor NSP-120–20-N) with a repetition rate of 1 kHz. The high voltage pulses were applied to a layer of 14 parallel tungsten rods, each with a length of 120 mm and diameter of 2 mm, which were separated by 6 mm. In a subjacent layer, at a distance of 6 mm, 15 more of these electrodes were arranged in a similar fashion but displaced horizontally by 3 mm with respect to the rods in the top layer. The electrodes in the bottom layer were enclosed in quartz tubes (4 mm diameter, 0.8 mm wall thickness) and grounded. In total, the chamber, containing the water mist, measured 120 × 120 mm at the base and 200 mm in height. The concept of the setup is shown in Fig. 2d. By pushing water with compressed air through a nebulizer with 50 mL min^{-1}, the operating medium, i.e. air, was saturated with water, including many small droplets. Moreover, water droplets that formed at the electrodes led to the plasma ignition primarily at the surface of the droplets. Hence, the water droplets were an integral part in the plasma generation process. To prevent heating of the CYN solution, it was kept at 18 °C in the circulation. Similar systems have, for example, already been investigated for the pollutant degradation of hospital wastewater [22,23].

2.7. Surface discharges at the air–water interface

The generation of discharges along a water surface, i.e. within the interface of the liquid to gas, was another investigated approach. The configuration was otherwise similar to the one for corona-like discharges in water. However, the reaction volume was filled only to a height of 35 mm with water (i.e. 32 mL) and the coaxial mesh electrode ended 10 mm beneath the water surface. Streamer discharges originated at the triple point (wire-water–air) from the two intertwined tungsten wires and propagated outwards along the surface when positive high

voltage pulses with an amplitude of 54.9 kV were applied from a 6-stage Marx-bank generator with a frequency of 20 Hz. The reactor measured 70 mm in height and 47 mm in diameter. The concept is shown in Fig. 2e. Since 50 μm tungsten wires did not sustain the extended generation of streamers from the same origin, they had to be replaced after 48 min by stronger wires of 80 μm for the second experiment. The CYN solution was moved with 50 mL min^{-1} and kept at 7 °C for the investigation. The configuration has been recently studied, for example, for the degradation of glyphosate in water [24].

2.8. Arc discharges in air

Arc discharges were generated in air in a rod-to-rod configuration with an electrode gap of 1 mm by supplying a 70 kHz AC high voltage with a peak-to-peak amplitude of 4 kV between the electrodes. The two tungsten rod electrodes, located beneath a nebulizer, were used to form an arc directly in the nebulized gas flow as shown in Fig. 2f. The solution, kept at 18 °C, was introduced to the reactor by compressed air and the treated liquid was then condensed in a 170 mm long PMMA tube with a diameter of 22 mm. Similar concepts have been used especially as gliding arc discharge configurations for the degradation of organic pollutants [25,26].

2.9. Plasma jet submerged in water

A plasma jet was expelled from a microhollow cathode discharge geometry, by applying a DC voltage of 500 V, resulting in a current of 30 mA, by pushing air through the electrode arrangement. The jet was submerged into the solution for good and immediate contact with the water and, due to the bubbling, a strong mixing of plasma-generated species with water was achieved, as shown in Fig. 2g. In this case, no water circulation or cooling was necessary (the solution maintained room temperature), and the entire volume of 200 mL was treated directly. The approach has so far primarily been studied for the inactivation of aqueous microorganisms [27,28].

3. Results

Six plasma processes were compared for their effectivity and efficiency to remove CYN. The different approaches can be distinguished according to their operating media and principles, i.e. discharges that were submerged in water, plasmas with the liquid as an integral part of the operation and the treatment of water with effluents from plasmas generated with air. For each category, two different principles with distinct characteristics were investigated. The selection was limited to approaches that can be exclusively operated in air or water and, do, in particular, not require noble gases. Therefore, these methods are, conceivably, the most relevant for an economic upscaling.

Prospective implementations of the technology depend foremost on degradation efficiencies but also on the absolute pollutant degradation on practical time scales with respect to actual needs (which might not require the complete removal). The respective decrease in CYN concentration with time is shown in Fig. 3 for the different configurations. Treatment times, $t_{0.9}$, that were required to achieve 90 % of CYN removal were extrapolated and are presented in Table 1. The corresponding reaction orders for the degradation of CYN were determined graphically, i.e. based on the goodness of fit for the integrated rate laws of zeroth (Equation (1)), first and second (Equation (2)) order reactions (also shown in Table 1 and in more detail in Supplementary Table S2). Accordingly, $t_{0.9,0th}$ or $t_{0.9,2nd}$ were estimated for zeroth and second order reactions from Equations (3) and (4), respectively.

$$c = c_0 - k_0 t \quad (1)$$

$$\frac{1}{c} = \frac{1}{c_0} + k_2 t \quad (2)$$

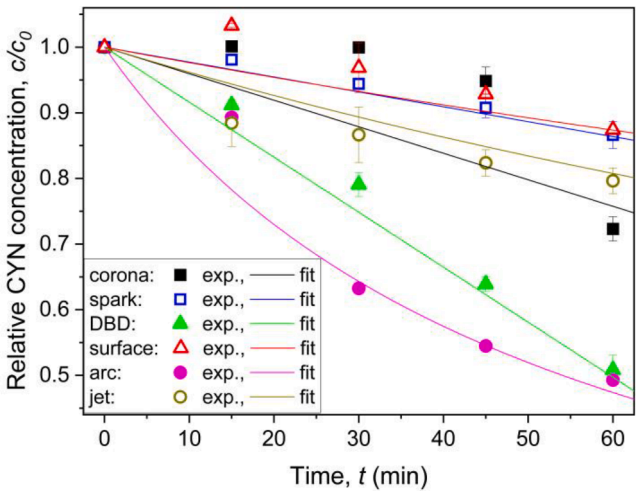

Fig. 3. Degradation of CYN with time for the treatment by the six investigated discharge configurations, i.e. corona-like discharges in water (corona), spark discharges in water (spark), DBD in humid air with immersed water droplets (DBD), surface discharges at the air–water interface (surface), arc discharges in air (arc) and plasma jet submerged in water (jet). The symbols show the measured data while the lines indicate the trends based on the reaction order and observed degradation rate constants as shown in Table 1. The initial CYN concentration was 0.3 μg mL^{-1} and experiments were repeated twice; error bars represent standard deviations.

$$t_{0.9,0th} = \frac{9 \times c_0}{10 \times k_0} \quad (3)$$

$$t_{0.9,2nd} = \frac{9}{c_0 \times k_2} \quad (4)$$

Here c_0 and c (in μg mL^{-1}) denote the initial CYN concentration and the concentration after treatment, k_0 (in μg mL^{-1} min^{-1}) and k_2 (in mL μg^{-1} min^{-1}) the observed rate constant for zeroth and second order, respectively, and t (in min) designates the actual treatment time.

Fig. 4 shows the energy that was dissipated by the different discharges with respect to the achieved CYN removal, corresponding to the different treatment times that are shown in Fig. 3. To assess the treatment efficiency, the electrical energy per order (E_{EO}), i.e. the electrical energy that was required for the removal of CYN by one order of magnitude (90 %), in 1 m^3 of polluted water, was estimated by Equation (5) (adapted from Bolton et al. [29]).

$$E_{EO}\ \left[kWh\ order^{-1}\ m^{-3}\right] = \frac{E \times 10^6}{V \times \log\left(\frac{c_0}{c}\right) \times 3{,}600} \quad (5)$$

The parameter E (in kJ) refers to the energy dissipated in the plasma, V (in mL) describes the treated volume, c_0 and c (in μg mL^{-1}) the initial and final CYN concentrations, respectively, and 10^6 and 3,600 are unit conversion factors. As a 90 % degradation of the toxin could not be achieved within 60 min of treatment by any of the investigated discharges (c.f. Fig. 3 and Table 1), the corresponding E_{EO} values were determined by extrapolating the experimentally obtained data assuming a first order reaction, as indicated by the term '$\log(c/c_0)$' in Equation (5), which is derived from the integrated rate law for first order reactions (refer to Bolton et al. [29] for a detailed explanation). The estimated E_{EO} values for the treatment of CYN by the six discharges are shown in Table 1. Although the measured data was best described by models of zeroth and second order reactions (c.f. Table 1), the differences in the goodness of fit (r^2) for the models of zeroth, first and second order reactions fitted to the experimental data was marginal for all six approaches, i.e. differed in the second decimal place at its worst (c.f. Supplementary Table S2). Accordingly, assuming a first order reaction is reasonable for the estimation of the E_{EO} values.

Table 1
Reaction orders and observed rate constants, k, as well as CYN removal after 60 min of treatment. The treatment time, $t_{0.9}$, that would be required for a 90 % degradation was determined according to the respective reaction order and the corresponding energy, E_{EO}, was extrapolated from rate constants assuming a pseudo first order reaction.

Discharge category	Discharge type	Reaction order	Observed rate constant (k) (goodness of fit (r^2))	CYN removal after 60 min of treatment in %	Time required to achieve 90 % CYN degradation ($t_{0.9}$) in min	Energy required for 90 % CYN degradation (E_{EO}) in kWh·order^{-1}·m^{-3}
Discharges in water	Corona	Pseudo 0th order	(1.1 ± 0.0) × 10^{-3} µg mL^{-1} min^{-1} (r^2 = 0.635 ± 0.062)	27.7 ± 0.0	222.7 ± 12.1	521.4 ± 50.2
	Spark	Pseudo 0th order	(0.7 ± 0.1) × 10^{-3} µg mL^{-1} min^{-1} (r^2 = 0.985 ± 0.005)	13.4 ± 0.0	400.3 ± 57.3	81.3 ± 13.6
Discharges at the air water interface	DBD	Pseudo 0th order	(2.6 ± 0.2) × 10^{-3} µg mL^{-1} min^{-1} (r^2 = 0.989 ± 0.006)	49.2 ± 0.0	107.5 ± 2.7	400.9 ± 38.4
	Surface	2nd order	(8.9 ± 1.3) × 10^{-3} mL µg^{-1} min^{-1} (r^2 = 0.728 ± 0.069)	12.6	3,781.5 ± 545.3	1,037.8
Discharges in air	Arc	2nd order	59.4 × 10^{-3} mL µg^{-1} min^{-1} (r^2 = 0.970)	50.7	486.7	406.8
	Jet	2nd order	(11.3 ± 1.4) × 10^{-3} mL µg^{-1} min^{-1} (r^2 = 0.868 ± 0.139)	17.6 ± 0.0	2,288.3 ± 300.8	± 82.8

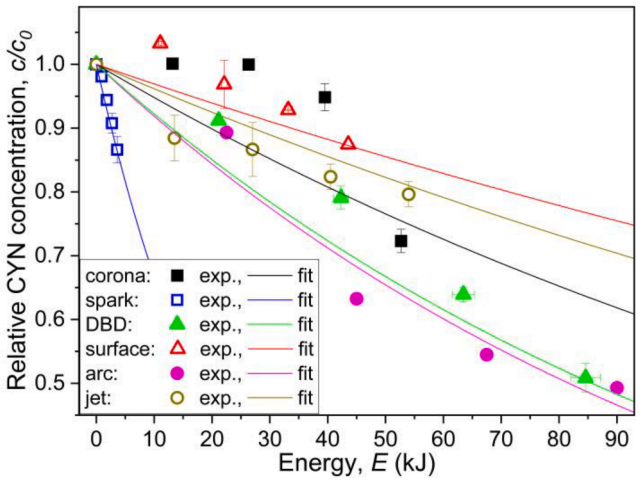

Fig. 4. Degradation of CYN in relation to the dissipated energy for the treatment by the six investigated discharge configurations, i.e. corona-like discharges in water (corona), spark discharges in water (spark), DBD in humid air with immersed water droplets (DBD), surface discharges at the air–water interface (surface), arc discharges in air (arc) and plasma jet submerged in water (jet). The symbols indicate the measured data while the lines indicate the trends assuming a pseudo first order reaction. The initial CYN concentration was 0.3 µg mL^{-1} and experiments were repeated twice; error bars represent standard deviations.

3.1. Individual degradation characteristics of different discharge configurations

3.1.1. Discharges submerged in water

One hour of treatment by the corona-like discharge submerged in water resulted in a degradation of CYN by 27.7 % for a provided energy of 52.7 kJ. Current and voltage measurements for a typical high voltage pulse that was applied with a frequency of 20 Hz are presented with the Supplementary Figure S7. Interestingly, degradation only started after an initial lag-phase of about 30 min as shown in Fig. 3. Fitting the degradation to a linear model, including the initial time lag, yielded the highest goodness of fit (r^2 = 0.635, c.f. Supplementary Table S2), which suggested a pseudo zeroth order reaction with respect to the decrease of the CYN concentration (Table 1).

After one hour of treatment by the spark discharge submerged in water, CYN was degraded by 13.4 % for a dissipated energy of 3.6 kJ. A linear relation of concentration with treatment time provided the best fit for the measurements (r^2 = 0.985, c.f. Supplementary Table S2), which indicated a pseudo zeroth order reaction kinetic (Table 1).

3.1.2. Discharges at the air–water interface

For the treatment by the DBD for one hour, CYN was degraded by 49.2 % with a dissipated energy of 84.6 kJ. Measurements for current and voltage for an individual applied high voltage pulse, repetitively applied with 1 kHz, are presented by Supplementary Figure S8. CYN degradation over time was best described by a linear relation (r^2 = 0.989, c.f. Supplementary Table S2), which indicated a pseudo zeroth order reaction with respect to the decrease of the CYN concentration (Table 1).

After one hour of treatment by the surface discharge, CYN was removed by 12.6 %, while in total 43.6 kJ were dissipated. Measurements for current and voltage for an individual applied high voltage pulse are shown with Supplementary Figure S9. CYN degradation started after an initial lag-phase of about 15 min (Fig. 3). A linear model, including the initial time lag, yielded the best fit (r^2 = 0.728, c.f. Supplementary Table S2) for reciprocal values of concentration versus treatment time, which indicated a second order reaction with respect to the decrease of the CYN concentration (Table 1).

3.1.3. Discharges in air

After one hour of treatment by the arc discharge, CYN was removed by 50.7 %. About 90.0 kJ were dissipated during this time. An exponential decrease of concentration was already observed for the treatment within 60 min (Fig. 3). Hence, the highest r^2 resulted from a linear model fitted to the reciprocal of the concentration plotted against the treatment time (r^2 = 0.970, c.f. Supplementary Table S2), which indicated a second order reaction with respect to the decrease of the CYN concentration (Table 1).

Treatment by the plasma jet resulted in 17.6 % CYN removal after one hour (Fig. 3). During the treatment 54.0 kJ were dissipated. CYN degradation by the plasma jet could be described by an exponential decrease with time (r^2 = 0.728, c.f. Supplementary Table S2), which indicated a second order reaction with respect to the decrease of the CYN concentration (Table 1).

3.2. Comparison of the discharge configurations

The six discharges were compared based on the total CYN removal as

well as the effectivity and efficiency described by the time and energy required to achieve 90 % of CYN removal, i.e. $t_{0.9}$ and E_{EO}, respectively. The total CYN removal after a treatment time of 60 min is shown in Fig. 5a. From this, the discharges could be ranked according to the CYN removal that was achieved as follows: arc (50.7 %) > DBD (49.2 %) > corona (27.7 %) > jet (17.6 %) > spark (13.4 %) > surface (12.6 %). Hence, the arc discharge and the DBD achieved the highest absolute toxin removal while the discharges in water, i.e. corona-like and spark discharges, or the surface discharge and the plasma jet were less effective. Although any degradation following a second order reaction was initially faster, the degradation rate eventually decreased and became infinitesimal small while the rate of the discharges for which the degradation followed a pseudo zeroth order reaction remained constant for the investigated treatment time as indicated in Fig. 3. The extrapolated trend of the degradation beyond the investigated treatment time of 60 min is shown more clearly by Supplementary Figure S10.

When the degradation efficacies were described by the time required to remove the toxin by 90 %, as it was expressed by the values for $t_{0.9}$ (Table 1), the order for a comparison of the performance changed: DBD (107.5 min) > corona (222.7 min) > spark (400.3 min) > arc (486.7 min) > jet (2,288.3 min) > surface (3,781.5 min). This is highlighted in Fig. 5b. Although the difference between the spark and arc discharges for a degradation of the toxin by 90 % was only about 87 min, it became obvious from the rate laws that discharges for which the degradation followed a second order reaction, i.e. arc, plasma jet and surface discharges, were less effective (c.f. Supplementary Figure S10). Especially for the plasma jet and surface discharge, the difference for required treatment times was substantial and the $t_{0.9}$ values by factors of about 22 and 36 higher than for the DBD.

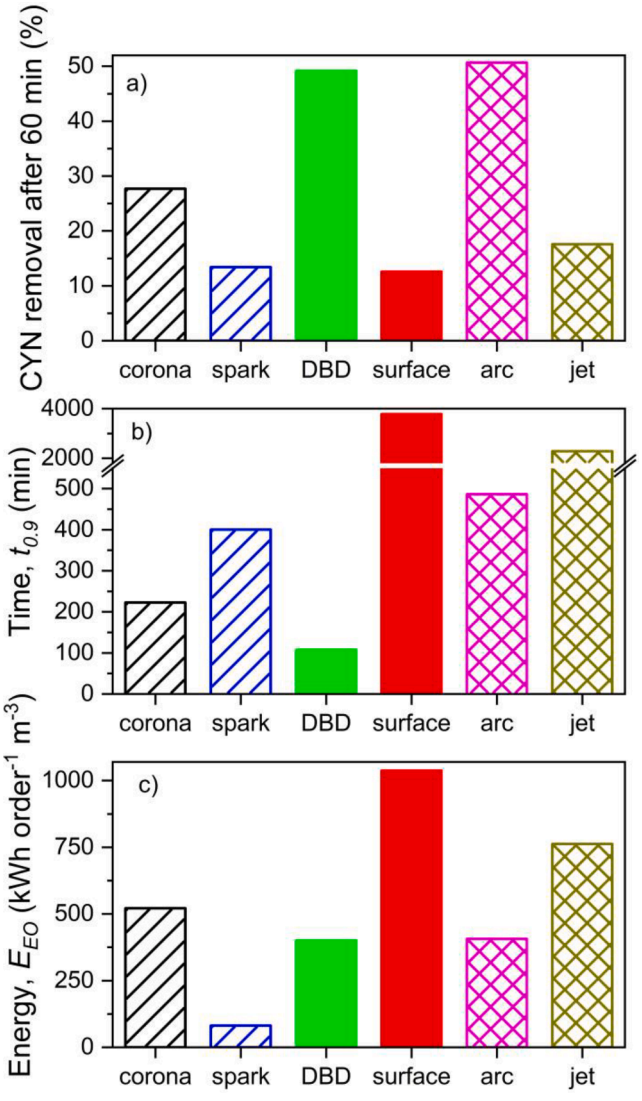

Fig. 5. Comparison of the six investigated discharge configurations, i.e. corona-like discharges in water (corona), spark discharges in water (spark), DBD in humid air with immersed water droplets (DBD), surface discharges at the air–water interface (surface), arc discharges in air (arc) and plasma jet submerged in water (jet): a) absolute CYN removal after 60 min of treatment, b) treatment time, $t_{0.9}$, required to achieve 90 % of CYN removal, and c) energy, E_{EO}, required to achieve 90 % of CYN removal in 1 m^{-3} of water (Table 1).

Although the treatment time is undoubtedly an important parameter, the processes' energy consumption becomes an essential parameter as well, especially when considering large-scale applications and related operating costs in addition to economical and societal efforts to decrease carbon footprints and to mitigate global warming. The overall energy consumption of a discharge can be related to the energy that was dissipated with the treatment. Hence, the E_{EO} values for the treatments (Table 1) were derived to assess the treatment efficiency of the discharges as shown in Fig. 5c. Under this aspect, the order for the more or less successful approaches changed: spark (81.3 kWh order^{-1} m^{-3}) > DBD (400.9 kWh order^{-1} m^{-3}) > arc (406.8 kWh order^{-1} m^{-3}) > corona (521.4 kWh order^{-1} m^{-3}) > jet (762.3 kWh order^{-1} m^{-3}) > surface (1,037.8 kWh order^{-1} m^{-3}).

A pseudo first order reaction, i.e. an exponential decrease in the CYN concentration, was assumed for the extrapolation of the E_{EO} values. Hence, the difference in the E_{EO} values was not affected by different reaction orders but solely by the degradation rate constant and the dissipated energy. The E_{EO} values describe, how efficient the energy that was dissipated in a discharge configuration was actually transferred effectively into the degradation of CYN. Of course, ideally a comprehensive degradation should be achieved both fast and with little energy. However, both constraints could apparently not be achieved simultaneously by a plasma treatment. For example, although the arc discharge and the DBD achieved a higher overall degradation (Fig. 5a), the spark discharge expended the provided energy about five times more efficiently (Fig. 5c). Likewise, the spark and arc discharges were more efficient than the corona-like discharge but would have required a substantially longer treatment to achieve 90 % of CYN removal (Fig. 5b and Fig. 5c, Table 1). Therefore, the method of choice has to be selected depending on the particular water treatment challenge, e.g. sustained protection of water reservoirs or immediate elimination of pollutants in drinking water, or high energy efficiency vs short treatment times.

4. Discussion

4.1. Characterization of plasma systems

The investigated typical plasma processes were based on electric discharges that can be operated in air and water without the need for further media, e.g. noble gases, or other consumables. The provided electrical energy is dissipated in different physical processes, i.e. strong electric fields, the ionization and electronic excitation of molecules and subsequent intense light emissions (radiation) and rapid local heating. Directly associated with these mechanisms were the generation of reactive oxygen and nitrogen species and local changes in pressure, e.g. shockwaves. The different channels, more or less pronounced, with resulting consequences on the degradation of chemical compounds, depended on specific system and plasma characteristics. In addition, these processes are the cause of electrode corrosion to a varying degree.

4.1.1. Comparison of physical attributes and constraints

A quantitative comparison of the intensity and magnitude of individual mechanisms for the different plasma systems was difficult. However, for the otherwise intentionally similar treatment conditions, e.g. treatment volumes (c.f. Fig. 2), a qualitative comparison was possible

and is described in more detail in section *4.1.2*. A qualitative comparison of the main aspects of different discharge configurations is summarized in Table 2.

An at least semi-quantitative guiding principle for the description of all processes that were provided by the different approaches together with respect to an observed result, e.g. the degradation of pollutants or the inactivation of microorganisms, can be provided by their active discharge volume. This parameter was estimated from the visible appearance of the plasma in the different systems and implied how effective the different physical processes that are described in Table 2 could be exploited. This included, in particular, the generation of short-lived atomic and molecular species. The parameter is further of interest for the operational requirements of an individual or multiple electrode configuration, e.g. electrical power, and to reveal limits for any related scaling. Due to practical and technical restraints, a precise determination of the active discharge volume could not be achieved. However, the expanse of the plasma within the reactor could be approximated and, in combination with the reactor dimensions and electrode geometry, allowed for estimations and comparisons at least to the nearest order of magnitude as shown in Table 3.

Although certain physical processes, e.g. the emitted radiation, could extend beyond the active discharge volume and, in particular, long-lived reactive species could be transported beyond this region, the interaction of the plasma-induced processes with pollutants and the generation of reactive species were expected to be the strongest within this volume and further determine their overall production. Therefore, the scalability of a particular method and the amount of water that can be treated simultaneously depends on the capacity to expand the active discharge volume. From the six investigated discharge configurations, the DBD and corona-like discharge are inherently scalable by extending the electrodes or electrode areas, whereas the active discharge volume of the other configurations could only be substantially increased by operating several similar systems in parallel. Accordingly, the latter would require a multiplication of electrical operating equipment while a direct extension of a discharge configuration offers the possibility of energy savings.

In this respect, the energy density of the investigated systems was calculated based on the estimated active discharge volume and the absolute energy that was dissipated by the plasma in 60 min of treatment (shown in Table 3). Notably, the arc and spark discharges had the highest energy density and thus, dissipated the most energy within the active discharge volume. Correspondingly, both configurations also provided a high degradation efficiency (c.f. Fig. 5c). Conversely, the DBD and corona-like discharge offered much larger active discharge volumes, although associated with the smallest energy densities. The trade-off still provided relatively high degradation yields (c.f. Fig. 5a). Despite having the largest active discharge volume, both configurations seemingly exploited the dissipated energy much more efficiently for processes that substantially contributed to the degradation of CYN, i.e. the generation of reactive chemical species. On the contrary, spark and arc discharges apparently dissipated a considerable amount of the energy for processes that were expected to only insignificantly contribute to the degradation of the toxin, e.g. high ion or gas temperatures (c.f. Table 2).

Table 3
Absolute energy dissipated by the plasma within 60 min of treatment, active discharge volume estimated to the nearest order of magnitude, calculated energy density of the active discharge volume for 60 min of treatment, and corresponding input power of the six discharge configurations.

Discharge category	Discharge type	Absolute energy dissipated by the plasma in 60 min of treatment in kJ	Active discharge volume (order of magnitude) in mm^3	Energy density after 60 min of treatment in $kJ \cdot mm^{-3}$	Input power in W
Discharges in water	Corona	52.7	1,000	0.05	14.6
	Spark	3.6	0.001	3,600.0	1.0
Discharges at the air–water interface	DBD	84.6	1,000	0.08	23.5
	Surface	43.6	100	0.44	12.1
Discharges in air	Arc	90.0	0.01	9,000.0	25.0
	Jet	54.0	1	54.0	15.0

4.1.2. Main physical characteristics of different discharge processes

The submerged corona-like plasma configuration promoted streamer discharges that were originating along the two intertwined wires towards the coaxially surrounding mesh electrode without bridging the electrode gap (Fig. 2c). The active discharge volume was, although densely, only partially filled with discharge filaments. Identifiable spectral lines for the emitted light were mainly found above 300 nm, e.g. $\cdot OH(A^2\sum^+ \rightarrow X^2\prod)$, H_α and H_β [30,31]. This was due to lower ion temperatures of about 1,800–2,200 K [32,33] in comparison to some of the other investigated discharges (c.f. Table 2). However, Lukes et al. [33] also observed radiation in the UV-C range. Additionally, the generation of shockwaves was reported [34,35], but the shear forces generated from the shockwaves could only affect a small area in close vicinity to the filaments [34].

Underwater spark discharges bridged the gap between the two sharpened rod electrodes with a single plasma channel (Fig. 2b). Similar to corona-like discharges, spark discharges have been reported to emit light in the spectral range from approximately 200 to 1,000 nm with an intensity of about one order of magnitude higher compared with the radiation produced by corona-like discharges [31]. The higher radiation intensity is related to the higher ion temperatures of several 10^3 to 10^4 K [20]. For the spark discharge reactor investigated in this study, Zocher et al. [21] assumed a temperature in the center of the spark channel of about 5,000 K, which readily decreased with distance from the discharge center to about 300 K at the plasma-water interface. Correspondingly, energy densities in this single discharge channel were much higher than for the filaments of the corona-like discharge in water [35]. The rapid heating of the spark is associated with the instigation of overpressures and shockwaves that were substantially stronger compared with the shockwaves generated by corona-like discharges in water. A pressure of about 500 MPa was estimated in close vicinity, i.e. 0.6 mm, from the spark discharge channel and was still about 140 MPa at a distance of 2.4 mm [21].

For the DBD reactor, the contaminated water was nebulized and

Table 2
Evaluation of the physical, i.e. radiative, thermal and mechanical processes, induced by the electric discharges (ranked from strongly developed to negligible for this discharge: "++" to "○").

Discharge category	Discharge type	Radiation	Temperature	Mechanical forces	Electrode corrosion
Discharges in water	Corona	+	+	+	++
	Spark	++	++	++	++
Discharges at the air–water interface	DBD	○	○	○	○
	Surface	○	○	○	+
Discharges in air	Arc	+	+	○	+
	Jet	○	○	○	○

sprayed into the discharge chamber where droplets formed at the top layer of high voltage electrodes and the quartz tubes, i.e. the dielectric material surrounding the bottom layer grounded electrodes. The water droplets could provide an additional dielectric barrier on both (Fig. 2d). The droplets moved along the electrodes and quartz tubes, grew in size, and eventually fell into the sample reservoir. Dielectric barrier discharge filaments that developed continuously often ended onto droplets and followed their movement, which constantly, but within relative small range, altered the active treatment volume. Due to the high repetition frequency of the applied voltage pulses, it can be assumed that the majority of droplets were treated. Therefore, the active volume was considered to be orders of magnitude larger compared to the active volumes of the spark and arc discharges (c.f. Table 3). Dielectric barrier discharges usually operate at temperatures closer to room temperature than spark and arc discharges, as even rotational ion temperatures remain below 1,000 K [36]. Hence, in contrast to the spark discharge, no broadband spectrum in the UV/Vis range could be observed and spectral emissions dominantly included molecular bands, e.g. for NO·, ·OH or N_2 [37].

The surface discharges resembled the streamer discharges formed in the corona-like plasma source, with the difference that the filamentous structure only appeared at the interface of air with water (Fig. 2e). Hence, interaction of the plasma with the operating media and reactive species production only occurred at this boundary. The active treatment volume resembled a disc with a radius smaller than the radius of the reactor. Although surface discharges also emitted UV light [38], the optical emission spectrum differed significantly from submerged corona-like plasmas and was similar to that of a DBD in air.

Similar to the spark discharge system, arc discharges connected two rod electrodes by a single plasma channel that was pushed out of the electrode gap due to the air flow (Fig. 2f). The discharge volume and the corresponding active plasma volume was approximately tenfold larger compared to the spark discharge (c.f. Table 3). However, while the spark discharge was immersed in water and, for the DBD, the entire nebulized volume of water was treated, only a fraction of the water spray was directly interacting with the arc. With gas temperatures in a similar range to the ion temperatures of a corona-like discharge (approximately 2,500 K), the arc afforded substantially lower temperatures compared to a spark discharge in water [39,40]. Besides the lower temperature, the intensity of light emitted by discharges in air was shown to be orders of magnitude lower than for discharges in water [41].

The plasma that was generated in the plasma jet was not getting into contact with the liquid directly. Instead the effluents were expelled under water by the air flow (Fig. 2g). Characteristic UV/Vis emissions, however, of low intensity, have been found for atmospheric air DC plasma jets with spectral lines, e.g. for atomic O and NO·, mainly at wavelengths above 300 nm [42,43]. Although the gas temperature in the discharge itself was in a range of about 10,000 K, it did not appear to correlate with the spectral emissions in the expelled plume [43]. Furthermore, due to effective cooling of the gas with the surrounding medium, the temperature readily dropped close to room temperature within a few millimeters from the discharge [27,42]. Hence, thermal and radiative processes were considered to be negligible [42]. More relevant were the reactive species that were released into water. Therefore, the active discharge volume was better described by the expelled afterglow plasma plume.

4.1.3. Classification of plasma chemical processes

The repeatedly expressed assumption that reactions with chemical species were the most important pathway for pollutant degradation by non-thermal plasmas was confirmed in our study [44–46]. For all of the investigated approaches, and plasmas generated from electric discharges in general, chemically reactive species originated from the excitation and ionization of atoms and molecules in the operating medium. Accountable processes are collisions with electrons but also photonic interactions, which result again in excitation, dissociation and ionization of molecules and atoms. These processes occur in a gaseous phase, which is present either directly as operating medium, e.g. air, or is established during the generation of a plasma. The latter applies, in particular, to discharges that are operated within the liquid. Especially reactive oxygen species (ROS) are formed in the absence of nitrogen while otherwise also reactive nitrogen species (RNS) are produced [47]. Due to fundamental similarities in the generation process, potent radicals that are initially formed with air or water are ·OH, ·H, O^{-}•, O_2^{-}•, HO_2•, NO•, NO_2• and NO_3• [44,47]. Production rates of these species depended on the specific characteristics of a discharge setup, e.g. temperatures, while their quantities depended particularly on the active discharge volume. Specifically the production of •OH is often pursued, also by other AOPs, for its significant oxidation potential. However, the life-time of this radical and also others are very short (e.g. considerably shorter than one second) and, therefore, require a direct interaction with any pollutant and a corresponding *in situ* generation. Conversely, longer-lived chemical species such as H_2O_2, O_3, nitrite (NO_2^{-}), nitrate (NO_3^{-}) or peroxynitrite ($ONOO^{-}$), formed by reactions of radicals with each other or constituents of the operating medium, are effective reagents, which can persist for several minutes or even days. Ambient conditions, e.g. temperature and water composition, need to be taken into account to describe their generation and decay. Their contribution to the degradation of pollutants can be significant and should not be omitted for the assessment of the efficacy and efficiency of a specific method. A respective overview of the generation of short- and long-lived reactive species by the different investigated concepts is summarized in Table 4.

A high amount of •OH was predominantly produced by electric discharges submerged in water, i.e. spark and corona-like discharges, while the generation of short-lived RNS and O_3 was considered negligible [48,49]. Higher •OH quantities were reported for spark discharges, due to higher energy densities in the single channel, in comparison to the •OH production in the individual filaments of a corona-like discharge [31]. The recombination of the short-lived •OH further yielded notable amounts of H_2O_2 for underwater discharges. Assuming a CYN degradation primarily by •OH (and subsequently formed species), this corresponded to the much lower E_{EO} value for the spark discharge presented in Fig. 5c. However, for the much larger active discharge volume of the corona-like discharge (c.f. Table 3), overall more •OH was provided and distributed in a larger treatment volume [50]. Consequently, CYN removal by submerged corona-like discharges exceeded the degradation by submerged spark discharges as described by Fig. 5a.

The degradation by •OH also played an important role for plasmas that were operated at the interface between air and water, i.e. the pulsed DBD and surface discharge [45,51]. Due to the available nitrogen, in addition, airborne RNS that dissolved into the liquid [45], provided further potential degradation pathways. These resulted in particular in the formation of $ONOO^{-}$, which could either directly take part in reactions or resulted in the indirect formation of •OH [52]. Because of the larger active discharge volume, respective processes were more dominant for the DBD due to the water droplets on the electrodes. Accordingly, both CYN removal and the E_{EO} value were considerably higher for this method than for the surface discharge with a much smaller surface

Table 4
Appraisal of the chemical processes, i.e. the generation of short- and long-lived reactive oxygen and nitrogen species, induced by the electric discharges (ranked from strongly developed to negligible for this discharge: "++" to "○").

Discharge category	Discharge type	Short-lived species		Long-lived species	
		ROS	RNS	ROS	RNS
Discharges in water	Corona	+	○	+	○
	Spark	++	○	+	○
Discharges at the air–water interface	DBD	+	+	++	+
	Surface	+	+	+	+
Discharges in air	Arc	○	++	○	+
	Jet	○	++	○	○

to treatment volume ratio (c.f. Fig. 5a and 5c). Interestingly, the combination of the different chemical processes for small separated water volumes, i.e. the water droplets, apparently provided distinct advantages in comparison to submerged corona-like and spark discharges.

The most prominent long-lived species that was confirmed especially for the DBD was O_3, which is in fact one of the foremost applications of this type of discharge [53]. Due to the high O_3-yield, in conjunction with the direct interaction with water droplets that were formed on the electrodes, subsequent reactions may have resulted again in more pronounced •OH-levels by processes similar to the submerged discharges.

For the arc discharge and the plasma jet that were both operated in air, the generation of short-lived species was dominated by RNS, e.g. NO•, NO_2• and NO_3•, while •OH was only formed in comparably negligible amounts at the interface with water [27,42,51]. Concurrently, the interaction with short-lived species was minimal for the water that was displaced by the already colder boundaries of the plasma jet. This effect can safely be assumed also for plasma jets that are operated with radiofrequency (rf) driven electrical excitations but are mostly operated with noble gases. These configurations are known for a significant production of ozone when operated in ambient air [54]. As the investigated plasma jet was operated with air in a microhollow cathode discharge configuration, reactions of nitrogen with oxygen outpaced the O_3 production. The accordingly primarily dissolved longer-lived species, including NO_2^-, NO_3^- and $ONOO^-$, were apparently not as effective for the degradation of CYN as more direct reactions with short-lived RNS. This was indicated by the much better CYN removal and lower E_{EO} value for the arc discharge as shown in Fig. 5a and 5c. Notably, the performance of this type of discharge, i.e. arc discharge, was similar to the treatment by the DBD, confirming the possibility of an effective CYN degradation even without significant amounts of •OH (c.f. Fig. 5a).

It should be remembered that the temperatures in the spark discharge channel and in the arc discharge are much higher than for the other investigated discharge plasmas. Consequently, the thermal cleavage of pollutants and of water, resulting in the formation of •OH [55], was a possibility. Likewise, high pressure gradients, i.e. shockwaves, could contribute to CYN degradation and •OH generation [20,55]. However, respective mechanisms would have been restricted to small regions in close vicinity to the discharge channels. Therefore, these processes were considered insignificant in comparison to reactions of CYN with chemical species.

The discussion shows that besides an efficient generation of reactive chemical species, their distribution and mixing within the treatment volume is of outmost importance. Obvious solutions, such as the mixing by a plasma jet, are not necessarily successful. The transport across the gas–liquid interface and within the liquid phase is an essential factor, which is determined by the species' lifespan and solubility as well as by the active discharge volume. A larger interaction volume can generally be assumed for longer-lived species but these species might not be the most effective for the degradation of pollutants. However, especially for short-lived reactive species, the transport through the solution or across the air–water boundary was a limiting process, which affected the actual interaction volume in which toxin degradation could still be achieved. Regardless, the comparison of the different approaches showed possibilities to further exploit and expand methods, such as for submerged spark discharges, or the potential of distributed volumes of water as demonstrated by the DBD operated in a water mist.

4.1.4. Electrode corrosion

The generation of reactive species and other plasma processes were unavoidably also responsible for the corrosion of the electrodes in the different discharge configurations. Besides the efficiency with respect to CYN degradation, corresponding implications might need to be considered for the further development and scaling of individual systems. The degree of electrode corrosion for the different discharge configurations is summarized in Table 2.

Regardless of the ground electrode material, Banaschik et al. [48] observed for the corona-like discharge electrode corrosion and release of iron or titanium from a stainless steel or a titanium ground electrode, respectively, in the lower mg L^{-1} range. Although they did not investigate the high voltage electrode, corrosion and tungsten release might occur here as well. The fact that the wire electrodes had to be replaced regularly during this study confirmed this assumption. Since the physical processes induced by the spark discharge were harsher compared with the corona-like discharge, the two tungsten rod electrodes were expected to be corroded to an at least similar degree. Consequently, the rod electrodes had to be sharpened again after a series of experiments to sustain the same operating conditions. As the setup of the arc discharges resembled the rod-to-rod geometry of the spark discharge, the electrodes may be expected to be corroded in the same fashion. However, since the physical processes induced by the arc discharge were less severe, i.e. lower thermal and mechanical stress, the electrodes were not expected to be affected as strongly. For the DBD, electrode corrosion should be less severe as the bottom layer is covered by the dielectric material and a major fraction of the discharges developed at the droplets formed on the electrodes but not the electrodes themselves. Due to the similar reactor design, corrosion of the grounded mesh electrode and the high voltage wire electrodes of the surface discharge could be expected to occur as it did in the corona-like discharge system. However, the concentration of released metals was expected to be substantially lower as the surface discharges developed only at the triple point of air, water and high voltage electrode while the corona-like discharges formed along the entire length of the high voltage electrode. Electrode and insulator corrosion during the operation of a plasma jet were shown to be insignificant [42].

The release of metals from the electrodes may generally have adverse implications for maintenance needs of the plasma reactor, the quality of the treated water and consequently, organisms that are exposed to the water. However, whether metal species released from the electrodes have adverse effects on organisms strongly depends, amongst other factors, on the released metal, its quantity, exposure time and the exposed organisms themselves. The electrodes used in the six investigated discharge configurations were either made of stainless steel, with iron being the main component, or tungsten. Iron is usually not considered to have detrimental health effects at these concentrations. In contrast, recent studies indicated that tungstate may cause adverse effects in different organisms [56,57] and therefore, the implementation of plasma-based water treatment may require additional efforts for removal.

4.2. Plasma-promoted toxin degradation

The ranking for the performance of the different discharge configurations differed depending on the applied criteria, i.e. absolute degradation, based on the time, $t_{0.9}$, required for a 90 % degradation of the toxin or dissipated energy (described in detail in section *3.2*). Note that the E_{EO} values were determined solely based on the energy dissipated by the plasmas, without considering energy demands by auxiliary supplies such as a pump to move the water through the reactor setups. For a large-scale implementation of the electrical discharge configurations, this would also need to be considered for the evaluation of the overall performance and energy efficiency. Regardless of the different criteria, the DBD operated in humid air with immersed water droplets provided an overall excellent performance. Corona-like discharges in water still offered competitive advantages with respect to absolute degradation and short treatment times. However, with respect to absolute degradation and energy efficiency, this concept was outperformed by arc discharges in air and spark discharges in water, respectively, despite their much smaller active volumes. Conversely, treatments with a plasma jet submerged in water or surface discharges at the air–water interface did not offer any competitive advantages. Responsible for the different rankings are the underlying processes of the individual approaches. These mechanisms are not unique to the degradation of the investigated

model pollutant, and, therefore, provide also instructive general insights for the treatment of recalcitrant compounds, in particular with similar chemical features, i.e. bonds, functional groups and solution characteristics.

4.2.1. Toxin susceptibility to physical plasma processes

Radiative, thermal, mechanical and chemical processes that were provided by the electric discharges were responsible for the degradation of the toxin. The different mechanisms have been described in section *4.1*. To what extent these processes played a part in the treatment depended on the physico-chemical properties of the pollutant itself but also on the water quality and composition.

Since many of the discharges delivered UV and also visible light (c.f. Table 2), photodegradation of pollutants was, in principle, possible. However, direct photodegradation of CYN at the investigated solution pH value of 5 has been shown to be ineffective, despite absorption maxima of CYN at wavelengths $\leq$ 200 nm and 262 nm [58–60]. Indirect photodegradation of CYN by visible light would require photosensitizers but not all cyanobacterial pigments act as photosensitizers [60,61]. Accordingly, direct and indirect photodegradation may have contributed to the overall decomposition of CYN but only to an insignificant degree.

Like many other toxins, CYN also appears to be persistent to thermal decomposition under conditions usually found in the environment, in water treatment facilities or in drinking water supply lines and households. The toxin was shown to be stable even at 100 °C at a pH value $\leq$ 7 [62]. As CYN remained dissolved in the water, a thermal decomposition could be achieved by discharges in direct contact with the solution, i.e. spark and corona-like discharges. While the spark discharges produced higher ion temperatures (c.f. Table 2), the corona-like discharges could have distributed the thermal energy across a larger active discharge volume (c.f. Table 3), affecting a higher quantity of CYN molecules. In addition, also arc discharges in air within the water spray provided temperatures inside the actual plasma channels that are most likely sufficient to decompose even recalcitrant pollutants (c.f. Table 2). But as the temperatures rapidly and substantially decreased within minuscule distances from the plasma channels for all these configurations, this process would have been limited to CYN in immediate vicinity to the discharges.

CYN is also an example for pollutants that are not susceptible to mechanical stress, justifiable due to its relatively low molecular mass of 415.4 g mol^{-1}. The mechanical stability is also illustrated by isolation techniques for CYN, which regularly employ sonication. As indicated in Table 2, only the discharges in water, i.e. spark and corona-like, were expected to generate shockwaves. The much stronger shockwaves produced by the spark discharges are sufficient for the disruption of algal cells [21] and assumingly also for cyanobacterial cells but unlikely to affect the toxin itself. Respective forces are also rapidly decreasing with distance from the plasma channel and, therefore, a relatively small fraction of the pollutant would come under their influence.

Also arc discharges in air within the water spray provided temperatures inside the actual plasma channels and, in their close vicinity, mechanical forces that are likely sufficient to decompose even the most recalcitrant pollutants. However, the corresponding active discharge volumes are rather small (c.f. Table 3) and, therefore, these mechanisms could not account for the observed ranking of the methods. Consequently, although physical processes may have contributed to the overall CYN degradation, the chemically-induced processes can be assumed to be primarily responsible for its degradation. Conversely, the degradation of compounds that are more susceptible than CYN to radiation, in particular to UV exposures, high temperatures or mechanical forces might be expedited by these physical processes in addition to the chemical decomposition.

4.2.2. Toxin degradation by reactive chemical species

The reactive species predominantly formed by electric discharges in air or water were ROS and RNS, especially •OH, H_2O_2 and O_3 as well as NO_x as described in section *4.1.3*. In general, •OH reacts non-selectively via an electrophilic attack on electron-rich moieties, via hydrogen abstraction from C—H—groups, and, at a neutral pH value via one-electron transfer. However, the latter is often kinetically disfavored and thus neglected [63]. In contrast to •OH, O_3 is more selective and primarily reacts with electron-rich moieties such as unsaturated C=C and C≡C bonds, aromatic systems and neutral amines [64]. The selectivity of the reactive species may have affected the treatment effectivity. For the diluted CYN extract, especially the short-lived reactive species in water, •OH, may have been more effectively scavenged by cyanobacterial cell residues. Although, the reactivity of •OH with CYN ($k_{\bullet OH} = 5.5 \times 10^9\ M^{-1}\ s^{-1}$ at a pH value of 7) was reported to be about four orders of magnitude higher than for O_3 ($k_{O3} = 3.4 \times 10^5\ M^{-1}\ s^{-1}$ at a pH value of 8) [65], concentrations of both species were an essential factor for the reaction with CYN. In comparison, CYN degradation by H_2O_2 was shown to be ineffective as less than 5 % of CYN was degraded within 500 min of treatment in the absence of light, i.e. without activation by UV irradiation [59]. Specific information on the reaction of CYN or any of its derivates with RNS was not found in the scientific literature. However, for short-lived RNS such as NO_3•, reaction mechanisms with organic compounds in water have been reported to be similar to •OH, i.e. hydrogen abstraction from saturated organic compounds, an electrophilic attack of double bonds in unsaturated organic compounds or electron transfer. Although NO_3• is more selective than •OH, available kinetics data for reactions of NO_3• with different organic molecules indicated that the radical is substantially less reactive than •OH [66]. On the contrary, long-lived RNS such as NO_2^- and NO_3^-, or their conjugated acids HNO_2 and HNO_3, were not expected to yield appreciable CYN degradation.

To summarize, the degradation of an organic compound depends not only on its quantity but, more importantly, on the actually produced reactive species and whether the compound features structural moieties that are susceptible to reactions, e.g. with •OH, O_3 or NO_3•. Due to its non-selective character, •OH has been found to react with numerous recalcitrant organic compounds. Contrarily, decomposition by the more selective O_3 requires electron-rich moieties, which makes O_3 ineffective for the degradation of a range of recalcitrant compounds. Principally, the production of •OH and, therefore, particularly discharges submerged in water may be considered the better choice as a broader range of organic compounds can be decomposed. However, due to its non-selective character, •OH is prone to scavenging by non-target compounds in the water such as natural organic matter, which, depending on the structure of the organic matter, can be a less severe issue for O_3.

Because of the substantially lower energy consumption, the spark discharge was about five times more efficient than the arc discharge and about six times more efficient than the corona-like discharge when considering the E_{EO} values (Table 1 and Fig. 5c). The results for the CYN degradation are in agreement with previously reported results on the degradation of other organic contaminants by spark and corona-like discharges [20]. This indicated that even though the degradation yield for the spark discharge was only about one fourth of the yield of the arc discharge and about half of the yield of the corona-like discharge (Table 1 and Fig. 5a), reactive species production and consequential CYN degradation by the spark discharge was more efficient in the smaller active volume.

Similar to the arc discharge, the investigated plasma jet mainly produced RNS (c.f. Table 4). However, the air flow that carried the produced reactive species also impeded their interaction with the solution. This could explain the lower treatment effectivity and efficiency (Table 1, Fig. 5b and Fig. 5c). Contrarily, in comparison with the surface discharge, the plasma jet yielded a higher CYN degradation, treatment effectivity and efficiency (Table 1 and Fig. 5). The more turbulent mixing of the plasma jet treatment may have resulted in a higher rate of encounters between reactive species and the toxin molecules.

Discharges at the air–water interface also produced •OH directly or

indirectly. The indirect radical generation was expected to be less pronounced compared to the discharges submerged in water because of poor O_3 solubility in water and the limited interaction of the plasma with the solution. The DBD-based treatment might have benefited from an acidification as dissolved ozone stability improves at lower pH values. Since the surface discharge at the air–water interface spread across the water surface, higher •OH quantities compared to the arc discharge could have been generated, which may have become effective only after pH values were lowered, non-target compounds sufficiently degraded first, or subsequent reaction products needed to be dispersed throughout the solution initially. This might explain the initial lag-phase that was also observed for the corona-like discharge. Even though the arc discharge was expected to mainly produce RNS while the DBD additionally produced higher levels of ROS (Table 4), the overall degradation yield and efficiency appeared to be within the same range (Table 1, Fig. 5a and Fig. 5c). However, due to the different reaction orders, the DBD would have needed only about one fourth of the time the arc discharge would have required to achieve a 90 % degradation (Table 1 and Fig. 5b).

Although the CYN solution treated by corona-like and surface discharges was kept at a 11 K lower temperature than the solution treated by the other discharges (c.f. section *2.3*), the difference of the solution temperature was not expected to have a substantial effect on the overall toxin degradation within this minor temperature range as was shown, e.g. for a comparable temperature range for the reaction of •OH with various organic compounds [67].

4.2.3. Degradation kinetics

Reactive species were continuously produced by all six discharges. For the short-lived reactive species, an equilibrium between their generation and consumption (including CYN degradation) was established early on during the treatment. The corresponding steady-state concentrations were species-specific and determined by the energy dissipated in the plasma for a particular configuration. Conversely, the concentration of long-lived reactive species might be assumed to continuously increase within the studied treatment time or until the treated water was saturated. In comparison, the CYN concentrations decreased with time. These characteristics were reflected by the pseudo zeroth order for CYN degradation, which could be determined for DBD, spark discharge and corona-like discharge (Table 1). However, CYN removal with the corona-like discharge started only after an initial lag-phase (c.f. Fig. 3). The most likely cause were cyanobacterial cell residues from the extract that initially scavenged the non-selective •OH more effectively than the more selective O_3, which was predominantly produced by the DBD. Conversely, cyanobacterial cell residues might have been readily decomposed with the spark discharges in the rather small treatment volume by the associated shockwaves. This concurs with previous observations for the disruption of microalgae [21]. Although the contribution of shockwaves to the degradation of the mechanically more stable CYN itself could be considered negligible, the process was apparently still relevant to substantially alleviate •OH scavenging.

On the contrary, CYN removal by the plasma jet, arc and surface discharges followed a second order reaction, i.e. a degradation depending on CYN concentrations together with reactive species concentrations. This indicated a restricted reaction of reactive species with the toxin, which was limited by the rate of encounters between the different molecules. Notably, the reactive species were generated in the gaseous phase for all the methods that can be described in this way. Hence, encounters between the dissolved toxin and reactive species were limited to reactions at the air–water surface and with reactive species that dissolved in the solution. Accordingly, the solubility of the originally gaseous species and their transport into and through the solution was a limiting factor.

An exception among the plasmas generated in the gaseous phase, i.e. with a CYN degradation following a pseudo zeroth order, was the treatment of the aerosolized solution by the DBD. In this case, the active plasma volume and, correspondingly, the interaction with the water was much larger and more comprehensive compared to the other discharges operated in the gas phase. In addition, the discharges also connected with the water droplets that formed on the electrodes. Therefore, exposure of CYN to the plasma and the reactive species, including higher O_3-yields, was more immediate and less dependent on transport processes. Conceivably, reactive species, such as •OH, were also indirectly formed from this interaction with water. This could similarly be assumed for the surface discharge across the water. However, the water mist provided a much larger total effective interface in comparison.

In principle, the turbulent mixing, which was achieved within the water mist with the arc discharge, should actually further improve the transfer of reactive species into the solution. Likewise, the plasma jet submerged in water afforded, at least in principle, better mixing and transport. The active discharge volumes were rather small for both the arc discharge and plasma jet, especially in comparison with the DBD and corona-like discharge. In addition, the transport of species from the gaseous phase into the liquid was conceivably impeded by the air flow, which carried the respective small molecules away before they could interact. Regardless, the plasma jet was still more efficient than the surface discharge for similar active discharge volumes (c.f. Table 3). Although, the absence of any turbulent mixing might be responsible for the initial lag-phase that was observed for the degradation of CYN by surface discharge treatment (c.f. Fig. 3).

The difference between pseudo zeroth and second order reactions was reflected by $t_{0.9}$ (Fig. 5b, Table 1). The time to achieve a CYN degradation by 90 %, i.e. $t_{0.9}$, was shorter for treatments with discharges that could be described by pseudo zeroth order reactions, shown by a linear decrease, while for the discharges for which the treatment followed a second order reaction, CYN decomposition followed an exponential decrease. Although the rate of a second order reaction may be faster in the beginning, it will gradually slow down while the rate of a pseudo zeroth order reaction remains constant throughout the treatment.

In contrast to the widely established ozonation as it is commonly realized, i.e. generation of O_3 by a DBD in an air or oxygen stream that is then bubbled through the water, the DBD operated in a water mist offered the advantage of a direct interaction of the electrical discharge with the gaseous and liquid phase at the same time. Although a comparison of treatment methods from distinct studies is often difficult due to experimental differences such as initial toxin and oxidant concentrations, solution pH and the water matrix, observed rate constants, determined for the six electrical discharges (c.f. Supplementary Table S2), were in the same order of magnitude compared to CYN treatment by 'common ozonation' under similar pH conditions [65]. This indicates that water treatment by electrical discharges is competitive to established treatment approaches such as ozonation.

5. Conclusion

The efficacies and efficiencies of six different approaches and corresponding electric discharge configurations were compared for the degradation of a recalcitrant toxic compound in water. With respect to economic technical implementations, the comparison was limited to methods that can be operated at atmospheric pressure in air or water without the need of other consumables. Degradation was investigated for CYN as a representative of the emerging threat by cyanotoxins, which have been shown to resist other, especially conventional, treatment approaches. As a model water pollutant, the characteristic of the toxin features sturdy (poly–)cyclic moieties and rather stable bonds, in particular unsaturated C═C double bonds, which provide stability also to many other substances that are problematic for water treatment. Thermal, mechanical and radiative processes induced by the plasmas might have directly or indirectly targeted the molecular structure and contributed to the overall CYN removal. Albeit, under the given conditions, the induced plasma-chemistry appeared to be the major driving

force for the degradation. Depending on the situation, i.e. type of pollutant as well as water quality and composition, different reactive species can be preferentially formed. In context of the quality of the treated water, questions may arise concerning electrode corrosion and the generation of NO_x, which could lead to an increase of undesired metal as well as nitrate and nitrite concentrations in water and may consequently require follow-up treatment. No electrode corrosion and, therefore, no trace metals were observed for the DBD but a nitrification. The submerged corona-like and spark discharges did not produce notable amounts of NO_x (from dissolved nitrogen), which were the predominant reaction products in other configurations that were operated in air.

Individual characteristics of the investigated systems and associated reaction pathways were responsible for their performance, which was expressed by different criteria. No single approach could unambiguously provide a comprehensive, fast and at the same time energy efficient treatment. Notably, the DBD operated in a water mist performed rather well with respect to all applied criteria and was at least the second best approach in every ranking. The submerged corona-like discharge also offered a still reasonable compromise between efficacy and efficiency, i.e. treatment time and energy demands, with the additional advantage that no NO_3^- or NO_2^- was formed. The actual implementation of the approaches further shows that these configurations are inherently scalable, i.e. the active discharge volume can be increased by extending electrodes or electrode areas. Conversely, for treatments with spark and arc discharges or a plasma jet, volumes can only be increased by the parallel operation of several similar systems.

In conclusion, different plasma treatment approaches may offer specific advantages for different situations, especially regarding operational conditions and constraints such as overall energy consumption, operating costs, residence time and with respect to water volumes that need to be treated in a certain time and the actual water composition. Which plasma process should be employed thus depends on the individual situation. If higher energy consumption is acceptable in exchange for shorter treatment times, the DBD offers the best treatment, especially if the treated water contains higher quantities of organic matter as O_3 is more selective than •OH. In contrast, if lower energy consumption is mandatory but treatment volumes are small or treatment times can be long, the spark discharge may be a better option.

Declaration of Competing Interest

The authors declare that they have no known competing financial interests or personal relationships that could have appeared to influence the work reported in this paper.

Data availability

Data will be made available on request.

Acknowledgement

This research received funding from the European Union's Horizon 2020 research and innovation programme under the Marie Sklodowska-Curie grant agreement No 722493, and was supported from the European Union's Horizon 2020 research and innovation programme under grant agreement No 857560. This publication reflects only the authors' view and the European Commission is not responsible for any use that may be made of the information it contains. The authors thank RECETOX RI (No LM2018121), financed by the Ministry of Education, Youth and Sports, and Operational Programme Research, Development and Innovation - project CETOCOEN EXCELLENCE (No CZ.02.1.01/0.0/0.0/17_043/0009632) for supportive background. We would like to thank Dr. Lucie Bláhová, Hana Klimová and Dr. Katja Zocher for their assistance and advice in the laboratory.

Appendix A. Supplementary data

Supplementary data to this article can be found online at https://doi.org/10.1016/j.cej.2022.138984.

References

[1] S. Mompelat, B. Le Bot, O. Thomas, Occurrence and fate of pharmaceutical products and by-products, from resource to drinking water, Environ. Int. 35 (2009) 803–814, https://doi.org/10.1016/j.envint.2008.10.008.
[2] N.H. Tran, M. Reinhard, K.-Y.-H. Gin, Occurrence and fate of emerging contaminants in municipal wastewater treatment plants from different geographical regions-a review, Water Res. 133 (2018) 182–207, https://doi.org/10.1016/j.watres.2017.12.029.
[3] G. Newcombe, International guidance manual for the management of toxic cyanobacteria, Global Water Research Coalition (2009). https://www.waterra.com.au/cyanobacteria-manual/PDF/GWRCGuidanceManualLevel1.pdf.
[4] R. Banaschik, P. Lukes, H. Jablonowski, M.U. Hammer, K.-D. Weltmann, J.F. Kolb, Potential of pulsed corona discharges generated in water for the degradation of persistent pharmaceutical residues, Water Res. 84 (2015) 127–135, https://doi.org/10.1016/J.WATRES.2015.07.018.
[5] V. Scholtz, J. Pazlarova, H. Souskova, J. Khun, J. Julak, Nonthermal plasma — A tool for decontamination and disinfection, Biotechnol. Adv. 33 (2015) 1108–1119, https://doi.org/10.1016/J.BIOTECHADV.2015.01.002.
[6] M. Magureanu, C. Bradu, V.I. Parvulescu, Plasma processes for the treatment of water contaminated with harmful organic compounds, J. Phys. D Appl. Phys. 51 (31) (2018) 313002.
[7] G.A. Codd, J. Meriluoto, J.S. Metcalf, Handbook of Cyanobacterial Monitoring and Cyanotoxin Analysis, in: J. Meriluoto, L. Spoof, G.A. Codd (Eds.), Handbook of Cyanobacterial Monitoring and Cyanotoxin Analysis, John Wiley & Sons, Ltd, Chichester, UK, 2016, pp. 1–8.
[8] M. Schneider, L. Bláha, Advanced oxidation processes for the removal of cyanobacterial toxins from drinking water, Environ. Sci. Eur. 32 (2020) 94, https://doi.org/10.1186/s12302-020-00371-0.
[9] J.-O. Jo, E. Jwa, Y.-S. Mok, Decomposition of Aqueous Anatoxin-a Using Underwater Dielectric Barrier Discharge Plasma Created in a Porous Ceramic Tube, Journal of the Korean Society of Water and Wastewater 30 (2016) 167–177, https://doi.org/10.11001/jksww.2016.30.2.167.
[10] B. Nisol, S. Watson, Y. Leblanc, S. Moradinejad, M.R. Wertheimer, A. Zamyadi, Cold plasma oxidation of harmful algae and associated metabolite BMAA toxin in aqueous suspension, Plasma Processes Polym. 16 (2019) 1800137, https://doi.org/10.1002/ppap.201800137.
[11] M. Schneider, R. Rataj, J.F. Kolb, L. Bláha, Cylindrospermopsin is effectively degraded in water by pulsed corona-like and dielectric barrier discharges, Environ. Pollut. 266 (2020), https://doi.org/10.1016/j.envpol.2020.115423.
[12] Y. Zhang, H. Wei, Q. Xin, M. Wang, Q. Wang, Q. Wang, Y. Cong, Process optimization for microcystin-LR degradation by Response Surface Methodology and mechanism analysis in gas–liquid hybrid discharge system, J. Environ. Manage. 183 (2016) 726–732, https://doi.org/10.1016/j.jenvman.2016.09.030.
[13] M.A. Malik, Water Purification by Plasmas: Which Reactors are Most Energy Efficient? Plasma Chem. Plasma Process. 30 (1) (2010) 21–31, https://doi.org/10.1007/s11090-009-9202-2.
[14] G.R. Stratton, C.L. Bellona, F. Dai, T.M. Holsen, S.M. Thagard, Plasma-based water treatment: Conception and application of a new general principle for reactor design, Chem. Eng. J. 273 (2015) 543–550, https://doi.org/10.1016/j.cej.2015.03.059.
[15] J.E. Foster, S. Mujovic, J. Groele, I.M. Blankson, Towards high throughput plasma based water purifiers: design considerations and the pathway towards practical application, J. Phys. D Appl. Phys. 51 (29) (2018) 293001.
[16] M. Saleem, O. Biondo, G. Sretenović, G. Tomei, M. Magarotto, D. Pavarin, E. Marotta, C. Paradisi, Comparative performance assessment of plasma reactors for the treatment of PFOA; reactor design, kinetics, mineralization and energy yield, Chem. Eng. J. 382 (2020), 123031, https://doi.org/10.1016/j.cej.2019.123031.
[17] L. Cerasino, J. Meriluoto, L. Bláha, S. Carmeli, T. Kaloudis, H. Mazur-Marzec, Extraction of Cyanotoxins from Cyanobacterial Biomass, in: J. Meriluoto, L. Spoof, G.A. Codd (Eds.), Handbook of Cyanobacterial Monitoring and Cyanotoxin Analysis, John Wiley & Sons, 2016, pp. 350–353.
[18] S. Yan, A. Jia, S. Merel, S.A. Snyder, K.E. O'Shea, D.D. Dionysiou, W. Song, Ozonation of Cylindrospermopsin (Cyanotoxin): Degradation Mechanisms and Cytotoxicity Assessments, Environ. Sci. Technol. 50 (2016) 1437–1446, https://doi.org/10.1021/acs.est.5b04540.
[19] M. Schneider, M.F. Grossi, D. Gadara, Z. Spáčil, P. Babica, L. Bláha, Treatment of cylindrospermopsin by hydroxyl and sulfate radicals: Does degradation equal detoxification? J. Hazard. Mater. 424 (2022), 127447 https://doi.org/10.1016/j.jhazmat.2021.127447.
[20] B. Sun, M. Sato, J.S. Clements, Oxidative Processes Occurring When Pulsed High Voltage Discharges Degrade Phenol in Aqueous Solution, Environ. Sci. Technol. 34 (2000) 509–513, https://doi.org/10.1021/es990024+.
[21] K. Zocher, R. Rataj, A. Steuer, K.-D. Weltmann, J.F. Kolb, Mechanism of microalgae disintegration by spark discharge treatment for compound extraction, J. Phys. D Appl. Phys. 53 (21) (2020) 215402.

[22] J. Kornev, N. Yavorovsky, S. Preis, M. Khaskelberg, U. Isaev, B.-N. Chen, Generation of Active Oxidant Species by Pulsed Dielectric Barrier Discharge in Water-Air Mixtures, Ozone Sci. Eng. 28 (4) (2006) 207–215.

[23] P. Ajo, S. Preis, T. Vornamo, M. Mänttäri, M. Kallioinen, M. Louhi-Kultanen, Hospital wastewater treatment with pilot-scale pulsed corona discharge for removal of pharmaceutical residues, J. Environ. Chem. Eng. 6 (2) (2018) 1569–1577, https://doi.org/10.1016/j.jece.2018.02.007.

[24] K. Zocher, P. Gros, M. Werneburg, V. Brüser, J.F. Kolb, P. Leinweber, Degradation of glyphosate in water by the application of surface corona discharges, Water Sci. Technol. 84 (5) (2021) 1293–1301, https://doi.org/10.2166/wst.2021.320.

[25] R. Burlica, M.J. Kirkpatrick, W.C. Finney, R.J. Clark, B.R. Locke, Organic dye removal from aqueous solution by glidarc discharges, J. Electrostat. 62 (4) (2004) 309–321, https://doi.org/10.1016/j.elstat.2004.05.007.

[26] C.M. Du, J.H. Yan, B.G. Cheron, Degradation of 4-Chlorophenol using a Gas-Liquid Gliding Arc Discharge Plasma Reactor, Plasma Chem. Plasma Process. 27 (5) (2007) 635–646, https://doi.org/10.1007/s11090-007-9092-0.

[27] X. Hao, A.M. Mattson, C.M. Edelblute, M.A. Malik, L.C. Heller, J.F. Kolb, Nitric Oxide Generation with an Air Operated Non-Thermal Plasma Jet and Associated Microbial Inactivation Mechanisms, Plasma Processes Polym. 11 (2014) 1044–1056, https://doi.org/10.1002/ppap.201300187.

[28] X. Pei, J. Kredl, X. Lu, J.F. Kolb, Discharge modes of atmospheric pressure DC plasma jets operated with air or nitrogen, J. Phys. D Appl. Phys. 51 (38) (2018) 384001.

[29] J.R. Bolton, K.G. Bircher, W. Tumas, C.A. Tolman, Figures-of-merit for the technical development and application of advanced oxidation technologies for both electric- and solar-driven systems (IUPAC Technical Report), Pure Appl. Chem. 73 (2001) 627–637, https://doi.org/10.1351/pac200173040627.

[30] B. Sun, M. Sato, J.S. Clements, Optical study of active species produced by a pulsed streamer corona discharge in water, J. Electrostat. 39 (1997) 189–202, https://doi.org/10.1016/S0304-3886(97)00002-8.

[31] B. Sun, M. Sato, A. Harano, J.S. Clements, Non-uniform pulse discharge-induced radical production in distilled water, J. Electrostat. 43 (1998) 115–126, https://doi.org/10.1016/S0304-3886(97)00166-6.

[32] P. Šunka, Pulse electrical discharges in water and their applications, Phys. Plasmas 8 (2001) 2587–2594, https://doi.org/10.1063/1.1356742.

[33] P. Lukes, M. Clupek, V. Babicky, P. Sunka, Ultraviolet radiation from the pulsed corona discharge in water, Plasma Sources Sci. Technol. 17 (2) (2008) 024012.

[34] R. Banaschik, G. Burchhardt, K. Zocher, S. Hammerschmidt, J.F. Kolb, K.-D. Weltmann, Comparison of pulsed corona plasma and pulsed electric fields for the decontamination of water containing Legionella pneumophila as model organism, Bioelectrochemistry 112 (2016) 83–90, https://doi.org/10.1016/J.BIOELECHEM.2016.05.006.

[35] K. Zocher, R. Banaschik, C. Schulze, T. Schulz, J. Kredl, C. Miron, M. Schmidt, S. Mundt, W. Frey, J.F. Kolb, Comparison of Extraction of Valuable Compounds from Microalgae by Atomspheric Pressure Plasmas and Pulsed Electric Fields, Plasma Medicine 6 (2016) 273–302, https://doi.org/10.1615/PlasmaMed.2017019104.

[36] K. Takashima (Udagawa), Y. Zuzeek, W.R. Lempert, I.V. Adamovich, Characterization of a surface dielectric barrier discharge plasma sustained by repetitive nanosecond pulses, Plasma Sources Sci. Technol. 20 (5) (2011) 055009.

[37] B. Chen, C. Zhu, J. Fei, X. He, C. Yin, Y. Wang, Y. Jiang, L. Chen, Y. Gao, Q. Han, Water Content Effect on Oxides Yield in Gas and Liquid Phase Using DBD Arrays in Mist Spray, Plasma Sci. Technol 18 (2016) 41–50, https://doi.org/10.1088/1009-0630/18/1/08.

[38] B.R. Locke, M. Sato, P. Sunka, M.R. Hoffmann, J.-S. Chang, Electrohydraulic Discharge and Nonthermal Plasma for Water Treatment, Ind. Eng. Chem. Res. 45 (2006) 882–905, https://doi.org/10.1021/ie050981u.

[39] A. Czernichowski, H. Nassar, A. Ranaivosoloarimanana, A. Fridman, M. Simek, K. Musiol, E. Pawelec, L. Dittrichova, Spectral and Electrical Diagnostics of Gliding Arc, Acta Phys. Pol. A 89 (1996) 595–603, https://doi.org/10.12693/APhysPolA.89.595.

[40] D.Z. Pai, G.D. Stancu, D.A. Lacoste, C.O. Laux, Nanosecond repetitively pulsed discharges in air at atmospheric pressure—the glow regime, Plasma Sources Sci. Technol. 18 (4) (2009) 045030.

[41] A.M. Anpilov, E.M. Barkhudarov, Y.B. Bark, Y.V. Zadiraka, M. Christofi, Y. N. Kozlov, I.A. Kossyi, V.A. Kop'ev, V.P. Silakov, M.I. Taktakishvili, S.M. Temchin, Electric discharge in water as a source of UV radiation, ozone and hydrogen peroxide, J. Phys. D Appl. Phys. 34 (2001) 993–999, https://doi.org/10.1088/0022-3727/34/6/322.

[42] J.F. Kolb, A.M. Mattson, C.M. Edelblute, X. Hao, M.A. Malik, L.C. Heller, Cold DC-Operated Air Plasma Jet for the Inactivation of Infectious Microorganisms, IEEE Trans. Plasma Sci. 40 (2012) 3007–3026, https://doi.org/10.1109/TPS.2012.2216292.

[43] Y. Xian, S. Wu, Z. Wang, Q. Huang, X. Lu, J.F. Kolb, Discharge Dynamics and Modes of an Atmospheric Pressure Non-Equilibrium Air Plasma Jet, Plasma Processes Polym. 10 (2013) 372–378, https://doi.org/10.1002/ppap.201200144.

[44] P.J. Bruggeman, M.J. Kushner, B.R. Locke, J.G.E. Gardeniers, W.G. Graham, D. B. Graves, R.C.H.M. Hofman-Caris, D. Maric, J.P. Reid, E. Ceriani, D. Fernandez Rivas, J.E. Foster, S.C. Garrick, Y. Gorbanev, S. Hamaguchi, F. Iza, H. Jablonowski, E. Klimova, J. Kolb, F. Krcma, P. Lukes, Z. Machala, I. Marinov, D. Mariotti, S. Mededovic Thagard, D. Minakata, E.C. Neyts, J. Pawlat, Z.L. Petrovic, R. Pflieger, S. Reuter, D.C. Schram, S. Schröter, M. Shiraiwa, B. Tarabová, P.A. Tsai, J.R.R. Verlet, T. von Woedtke, K.R. Wilson, K. Yasui, G. Zvereva, Plasma–liquid interactions: a review and roadmap, Plasma Sources Sci. Technol. 25 (5) (2016), 053002, https://doi.org/10.1088/0963-0252/25/5/053002.

[45] P. Lukeš, Water treatment by pulsed streamer corona discharge (Ph.D. Thesis), Department of Water Technology and Environmental Engineering, University of Chemistry and Technology, Prague, Czech Republic (2001). http://old.ipp.cas.cz/Ips/public/lukes_dissert.pdf.

[46] E.E. Rodriguez, W.A. Tarpeh, K.R. Wigginton, N.G. Love, Application of plasma for the removal of pharmaceuticals in synthetic urine, Environ. Sci. Water Res. Technol. 8 (3) (2022) 523–533, https://doi.org/10.1039/D1EW00863C.

[47] P. Lukes, E. Dolezalova, I. Sisrova, M. Clupek, Aqueous-phase chemistry and bactericidal effects from an air discharge plasma in contact with water: evidence for the formation of peroxynitrite through a pseudo-second-order post-discharge reaction of H2O2 and HNO, Plasma Sources Sci. Technol. 23 (1) (2014), 015019, https://doi.org/10.1088/0963-0252/23/1/015019.

[48] R. Banaschik, P. Lukes, C. Miron, R. Banaschik, A.V. Pipa, K. Fricke, P.J. Bednarski, J.F. Kolb, Fenton chemistry promoted by sub-microsecond pulsed corona plasmas for organic micropollutant degradation in water, Electrochim. Acta 245 (2017) 539–548, https://doi.org/10.1016/J.ELECTACTA.2017.05.121.

[49] K. Zocher, J.-W. Lackmann, J. Volzke, L. Steil, M. Lalk, K.-D. Weltmann, K. Wende, J.F. Kolb, Profiling microalgal protein extraction by microwave burst heating in comparison to spark plasma exposures, Algal Research 39 (2019), 101416, https://doi.org/10.1016/j.algal.2019.101416.

[50] R. Banaschik, H. Jablonowski, P.J. Bednarski, J.F. Kolb, Degradation and intermediates of diclofenac as instructive example for decomposition of recalcitrant pharmaceuticals by hydroxyl radicals generated with pulsed corona plasma in water, J. Hazard. Mater. 342 (2018) 651–660, https://doi.org/10.1016/J.JHAZMAT.2017.08.058.

[51] O. Lesage, L. Falk, M. Tatoulian, D. Mantovani, S. Ognier, Treatment of 4-chlorobenzoic acid by plasma-based advanced oxidation processes, Chem. Eng. Process. Process Intensif. 72 (2013) 82–89, https://doi.org/10.1016/J.CEP.2013.06.008.

[52] J.W. Coddington, J.K. Hurst, S.V. Lymar, Hydroxyl Radical Formation during Peroxynitrous Acid Decomposition, J. Am. Chem. Soc. 121 (1999) 2438–2443, https://doi.org/10.1021/ja982887t.

[53] J. Meichsner, M. Schmidt, R. Schneider, H.E. Wagner, Selected Applications, Nonthermal Plasma Chemistry and Physics, CRC Press, Boca Raton, 2013, pp. 285–406.

[54] A. Schmidt-Bleker, R. Bansemer, S. Reuter, K.-D. Weltmann, How to produce an NOx- instead of Ox-based chemistry with a cold atmospheric plasma jet, Plasma Processes Polym. 13 (11) (2016) 1120–1127, https://doi.org/10.1002/ppap.201600062.

[55] W. Song, T. Teshiba, K. Rein, K.E. O'Shea, Ultrasonically Induced Degradation and Detoxification of Microcystin-LR (Cyanobacterial Toxin), Environ. Sci. Technol. 39 (2005) 6300–6305, https://doi.org/10.1021/es048350z.

[56] W.C. McCain, L.C.B. Crouse, M.A. Bazar, L.E. Roszell, G.J. Leach, J.R. Middleton, G. Reddy, Subchronic Oral Toxicity of Sodium Tungstate in Sprague-Dawley Rats, International Journal of Toxicology 34 (4) (2015) 336–345, https://doi.org/10.1177/1091581815585568.

[57] O. Wasel, J.L. Freeman, Comparative Assessment of Tungsten Toxicity in the Absence or Presence of Other Metals, Toxics 6 (4) (2018), https://doi.org/10.3390/toxics6040066.

[58] K.-I. Harada, I. Ohtani, K. Iwamoto, M. Suzuki, M.F. Watanabe, M. Watanabe, K. Terao, Isolation of cylindrospermopsin from a cyanobacterium Umezakia natans and its screening method, Toxicon 32 (1994) 73–84, https://doi.org/10.1016/0041-0101(94)90023-X.

[59] X. He, A.A. de la Cruz, D.D. Dionysiou, Destruction of cyanobacterial toxin cylindrospermopsin by hydroxyl radicals and sulfate radicals using UV-254 nm activation of hydrogen peroxide, persulfate and peroxymonosulfate, J. Photochem. Photobiol., A 251 (2013) 160–166, https://doi.org/10.1016/J.JPHOTOCHEM.2012.09.017.

[60] M. Adamski, P. Żmudzki, E. Chrapusta, A. Kaminski, B. Bober, K. Zabaglo, J. Bialczyk, Characterization of cylindrospermopsin decomposition products formed under irradiation conditions, Algal Research 18 (2016) 1–6, https://doi.org/10.1016/J.ALGAL.2016.05.027.

[61] R.K. Chiswell, G.R. Shaw, G. Eaglesham, M.J. Smith, R.L. Norris, A.A. Seawright, M.R. Moore, Stability of cylindrospermopsin, the toxin from the cyanobacterium, Cylindrospermopsis raciborskii: Effect of pH, temperature, and sunlight on decomposition, Environ. Toxicol. 14 (1999) 155–161, https://doi.org/10.1002/(SICI)1522-7278(199902)14:1<155::AID-TOX20>3.0.CO;2-Z.

[62] M. Adamski, P. Żmudzki, E. Chrapusta, B. Bober, A. Kaminski, K. Zabaglo, E. Latkowska, J. Bialczyk, Effect of pH and temperature on the stability of cylindrospermopsin, Characterization of decomposition products, Algal Research 15 (2016) 129–134, https://doi.org/10.1016/J.ALGAL.2016.02.020.

[63] C. von Sonntag, U. von Gunten, Reactions of hydroxyl and peroxyl radicals, Chemistry of Ozone in Water and Wastewater Treatment: From Basic Prinicples to Applications, IWA Publishing, London (2012) 225–248, https://doi.org/10.2166/9781780400839.

[64] J.A. Westrick, D.C. Szlag, B.J. Southwell, J. Sinclair, A review of cyanobacteria and cyanotoxins removal/inactivation in drinking water treatment, Anal. Bioanal. Chem. 397 (2010) 1705–1714, https://doi.org/10.1007/s00216-010-3709-5.

[65] G.D. Onstad, S. Strauch, J. Meriluoto, G.A. Codd, U. Von Gunten, Selective oxidation of key functional groups in cyanotoxins during drinking water ozonation, Environ. Sci. Technol. 41 (2007) 4397–4404, https://doi.org/10.1021/es0625327.
[66] N.L. Ng, S.S. Brown, A.T. Archibald, E. Atlas, R.C. Cohen, J.N. Crowley, D.A. Day, N.M. Donahue, J.L. Fry, H. Fuchs, R.J. Griffin, M.I. Guzman, H. Herrmann, A. Hodzic, Y. Iinuma, J.L. Jimenez, A. Kiendler-Scharr, B.H. Lee, D.J. Luecken, J. Mao, R. McLaren, A. Mutzel, H.D. Osthoff, B. Ouyang, B. Picquet-Varrault, U. Platt, H.O.T. Pye, Y. Rudich, R.H. Schwantes, M. Shiraiwa, J. Stutz, J. A. Thornton, A. Tilgner, B.J. Williams, R.A. Zaveri, Nitrate radicals and biogenic volatile organic compounds: oxidation, mechanisms, and organic aerosol, Atmos. Chem. Phys. 17 (2017) 2103–2162, https://doi.org/10.5194/acp-17-2103-2017.
[67] B. Ervens, S. Gligorovski, H. Herrmann, Temperature-dependent rate constants for hydroxyl radical reactions with organic compounds in aqueous solutions, PCCP 5 (9) (2003) 1811–1824, https://doi.org/10.1039/B300072A.